Unusual Properties of Convection and Dynamos in Rotating Spherical Shells

F. H. Busse[1, *]

[1] *Institute of Physics, University of Bayreuth, D-95440 Bayreuth, Germany*

Convection in rotating spherical fluid shells is the basic dynamical process in the description of heat transports in planets and in stars. Since the respective fluids are often electrically conducting, the occurrence of convection is frequently associated with the generation of magnetic fields. The interaction between velocity and magnetic fields gives rise to rich dynamical structures in dependence on the numerous parameters of the problem.

PACS numbers:

I. INTRODUCTION

The interest in the problem of convection in rotating spheres has been stimulated by its astrophysical applications and by the search for the origin of geomagnetism in the Earth's liquid outer core. The exploration of the solar system and the discovery of the magnetic fields of other planets has amplified this interest and in the past decades a large number of papers dealing with convection in fluid shells and its dynamo action have appeared. Instead of reviewing all of this work we wish just wish to draw the attention to a number of surprising features that have appeared in the course of this work and which are of more general interest in the field of fluid dynamics. In order to make this article more readily accessible to a general resdership the use of mathematical equations and formulas is minimized. For more complete introductions to the subject we refer to the book [1] and the review article [5].

II. THERMAL ROSSBY WAVES

A basic theorem of the dynamics of rotating fluids is the Proudman-Taylor theorem which states that steady small amplitude motions of a barotropic rotating fluid do not vary in the direction of the axis of rotation when viscous effects can be neglected. "Small amplitude" means in this connection that the vorticity of the motion is negligible in comparison to the rotation rate of the system. The Proudman-Taylor condition is a consequence of the complete balance between Coriolis force and pressure gradient. This balance is also called geostrophic balance since it holds in good approximation for the large scale motions in the Earth's atmosphere.

Two-dimensional fluid motions can not often be accommodated in physical reality and in a spherical shell in particular two-dimensional motions are prevented by the boundary conditions. Fluid flows are thus forced to become time dependent. In the simplest cases the motions assume the form of nearly two-dimensional propagating Rossby waves. As indicated in figure 1, Rossby waves can be understood on the basis of the conservation of angular momentum. When a column of fluid (aligned with the axis of rotation) moves into a shallower place it becomes compressed and - because of the conservation of mass - its moment of inertia increases. To conserve angular momentum its rotation relative to an inertial frame of reference must decrease. Relative to the rotating system it thus acquires anticyclonic vorticity. The opposite process happens when the column moves to a deeper place where it gets stretched in the direction of the axis of rotation and acquires cyclonic vorticity.

In the annular fluid layer of figure 1 the depth decreases with increasing distance from the axis. A sinusoidal displacement of the initially static fluid columns leads to a flow structure in the form of vortices which tend to move the columns to new positions as indicated by the dashed line in the lower plot of the figure, i.e. the initial sinusoidal displacement propagates as a wave in the prograde direction. A retrograde propagation relative to the sense of rotation will be obtained when the depth of the annular layer increases with distance from the axis.

Rossby waves Like water waves Rossby waves decay, of course, when there is no force sustaining them against viscous dissipation. The possibility for such a sustenance exists in a thermally unstably stratified system where thermal Rossby waves may be generated. Growing disturbances are obtained in an annular configuration as sketched in figure 2 when a temperature difference, $T_2 - T_1$, and a gravity force are applied in the x-direction. In the experimental realization of the problem [2] the centrifugal force $\Omega^2 r_0$ is used as gravity and the temperature gradient must point outward in order

---

*Electronic address: busse@uni-bayreuth.de

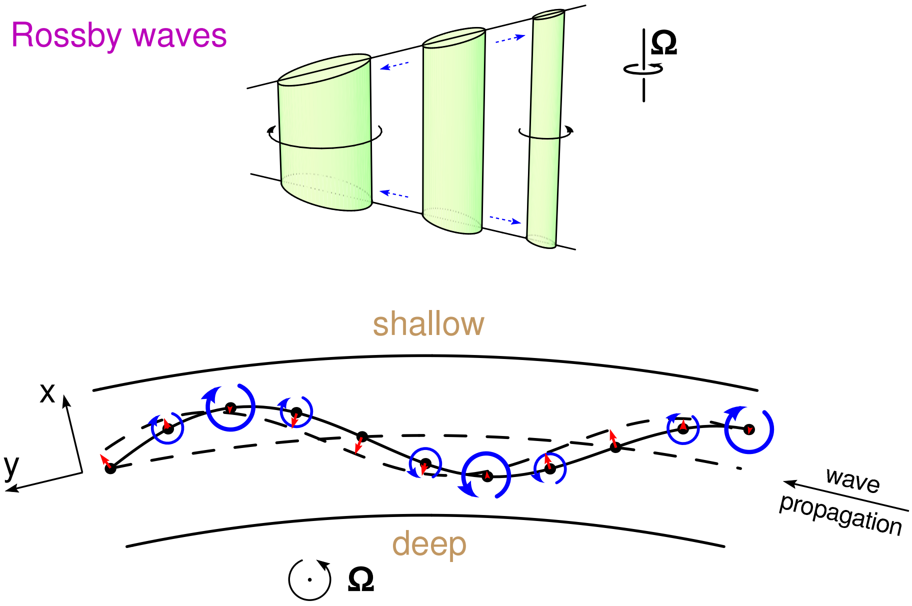

FIG. 1: Sketches for the dynamics of Rossby waves

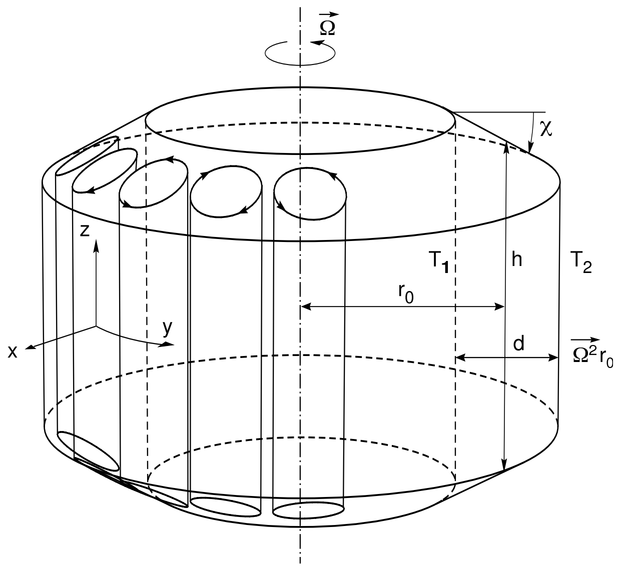

FIG. 2: Geometrical configuration of the rotating annulus.

to create the unstable density stratification. For geophysical applications one may think of the opposite directions for gravity and temperature gradient, but the mathematical problem remains the same in both cases.

The annulus configuration of figure 2 may be regarded as an annular section of a rotating spherical shell. Indeed, the theory developed for the rotating annulus can be applied in good approximation to the case of convection in a self-gravitating rotating fluid sphere heated from within [3]. As a standard model a spherical fluid shell of thickness d rotating with a constant angularvelocity Ω is often assumed for which a static state exists when thetemperature depends only on the distance from the center. Here we shall assume the particular temperature distribution $T_S = T_0 - \beta d^2 r^2/2$ which corresponds to a homogeneously heated sphere. rd isthe length of the position vector, $\vec{r}$, with respect to the center of thesphere and the gravity field is assumed in the form $\vec{g} = -d\gamma\vec{r}$. Usingthe length d, the time d^2/ν and the temperature $\nu^2/\gamma\alpha d^4$ dimensionless equations can be formulated in which the Rayleigh number R, the

FIG. 3: Convection columns in a rotating spherical fluid shell for $\tau = 10^4, R = 3.8 \cdot 10^5, P = 1$. Dark and light surfaces correspond to a constant positive and negative value of the radial velocity.

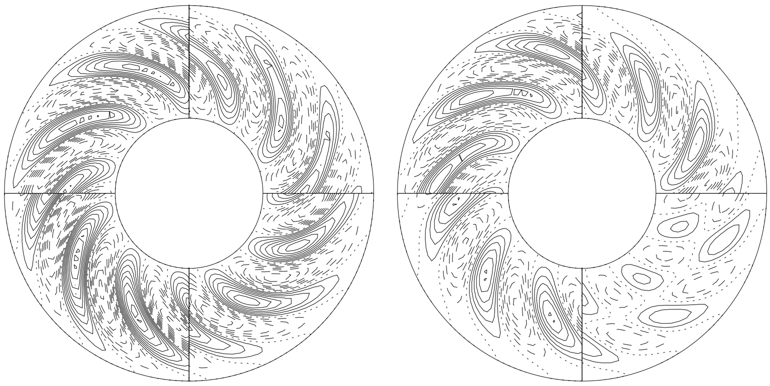

FIG. 4: Time periodic vacillations of convection at $Ra = 2.8 \times 10^5$ (left side) and $Ra = 3 \times 10^5$ (right side) for $\tau = 10^4$, $Pr = 1$ The streamlines, $r\partial u_p/\partial\varphi =$ const. are shown in one quarter of the equatorial plane. The four quarters are equidistant in time (with $\Delta t = 0.015$ ($\Delta t = 0.024$) in the left (right) case in the clockwise sense such that approximately a full period is covered by the circles.

Coriolis number τ and the Prandt lnumber P,

$$R = \frac{\alpha\gamma\beta d^6}{\nu\kappa}, \ \ \tau = \frac{2\Omega d^2}{\nu}, \ \ P = \frac{\nu}{\kappa}, \tag{1}$$

appear as dimensionless parameters. Here ν denotes the kinematic viscosity of the fluid, κ its thermal diffusivity, ϱ its density and α is the coefficient of thermal expansion. Since the Boussinesq approximation is assumed, the velocity field $\vec{u}$ is solenoidal and the general representation in terms of poloidal and toroidal components can be used,

$$\vec{u} = \nabla \times (\nabla v \times \vec{r}) + \nabla w \times \vec{r} \ , \tag{2}$$

such that the radial velocity depends on v alone and is given by $u_r = L_2 v \equiv \partial^2 ru/\partial r^2 - r\nabla^2 v$. A typical picture of thermal Rossby waves in a rotating spherical fluid shell is shown in figure 3. Here as well as in the following the ratio 0.4 between inner and outer radius of the shell has been used. Because of the symmetry of the progradely propagating velocity field with respect to the equatorial plane it is sufficient to plot streamlines in this plane, given by $r\partial v/\partial r = const.$, in order to characterize the convection flow as has been done in figures 4, 5 and 6. Even in the case of turbulent convection the part of the velocity field that is antisymmetric with respect to the equatorial plane is rather small.

As the Rayleigh number R increases beyond its critical value R_c for the onset of convection in the form of thermal Rossby waves, a sequence of bifurcations can be observed similar to those found in other problems of convection. First, typical oscillations in amplitude are observed as shown in figure 4, then another bifurcation may add low wavenumber modulations in the azimuthal direction as shown in figure 5. Finally, a chaotic state of convection is obtained.

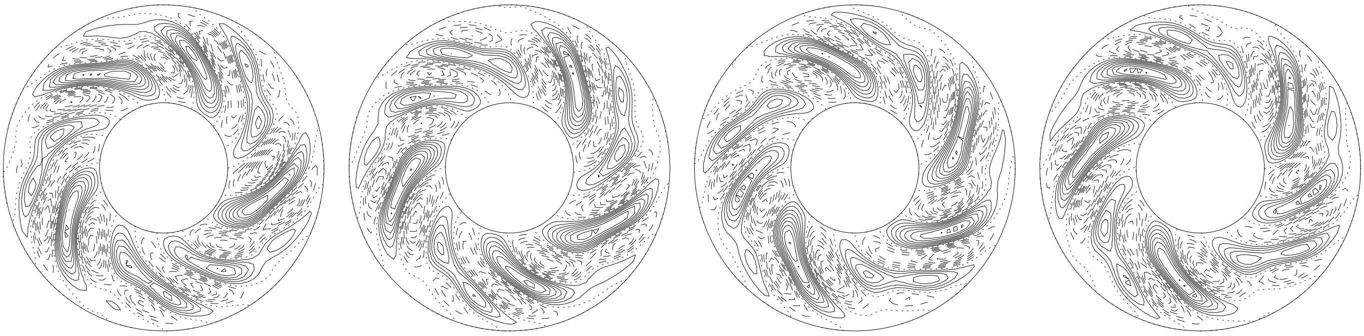

FIG. 5: Modulated shape vacillations of convection for $Ra = 2.9 \times 10^5$, $\tau = 10^4$, $Pr = 1$. The plots show streamlines, $r\frac{\partial u_p}{\partial \phi} = const.$, in the equatorial plane and are equidistant in time with $\Delta t = 0.04$ so that approximately a full period is covered.

III. CHAOTIC CONVECTION IN ROTATING SPHERICAL SHELLS

The sequence of transitions is also evident in the time dependence of average quantities such as the convective heat transport plotted in figure 6. The latter is described by the Nusselt number which is defined as ratio between the average gradients of the temperature at the inner boundary of the shell in the presence of convection and in its absence. Also of interest are the components of the kinetic energy density which are defined by

$$E_p^m = \frac{1}{2}\langle \mid \nabla \times (\nabla \bar{v} \times \vec{r}) \mid^2 \rangle, \quad E_t^m = \frac{1}{2}\langle \mid \nabla \bar{w}_t \times \vec{r} \mid^2 \rangle \tag{3a}$$

$$E_p^f = \frac{1}{2}\langle \mid \nabla \times (\nabla \check{v}_p \times \vec{r}) \mid^2 \rangle, \quad E_t^f = \frac{1}{2}\langle \mid \nabla \check{w}_t \times \vec{r} \mid^2 \rangle \tag{3b}$$

where the angular brackets indicate the average over the fluid shell and where $\bar{v}_p$ refers to the azimuthally averaged component of v_p and $\check{v}_p$ is given by $\check{v}_p = v_p - \bar{v}_p$. E_t^m describes the energy density of the differential rotation which increases substantially with increasing R as is evident from figure 6. This increase is caused by the strong Reynolds stress of the convection eddies resulting from their inclination with respect to radial direction which is evident in figures 3 through 5. The shear of the differential rotation, however, tends to inhibit convection in that it shears off the convection eddies. This is a consequence of the nearly two-dimensional nature of the dynamics in a rotating system: In a non-rotating system the convection rolls would simply align themselves with the direction of the shear and the heat transport would thus remain unchanged. In the rotating sphere a precarious balance results realized in the form localized convection. As shown in figure 7 convection occurs only in a restricted azimuthal section of the spherical shell where its amplitude is sufficiently strong to overcome the inhibiting influence of the shear. The axisymmetric differential rotation continues to be driven by the localized convection. The advection by the differential rotation of the thermal boundary layers which have expanded in the non-convecting region of the shell actually strengthens the localized convection in that its available buoyancy is replenished.

Instead of a spatial localization the localization of convection in time offers another possibility for the precarious balance as demonstrated in figures 8 and 9. Here convection exist only for a short period while the differential rotation is sufficiently weak. As the amplitude of convection grows the differential rotation grows even more strongly as the Reynolds stress increases with the square of the amplitude. Soon the shearing action becomes strong enough to cut off convection. Now a viscous diffusion time must pass before the differential rotation has decayed sufficiently such that convection may start growing again. It is remarkable to see how the chaotic system exhibits its nearly periodic relaxation oscillations as shown in figure 8.

The convective heat transport in the case of localized convection as well as in the case of the relaxation oscillations is, of course, much reduced relative to a case without strong differential rotation. Here the magnetic field enters in an important way. By putting the brakes on the differential rotation through its Lorentz force the magnetic field permits a much higher heat transport than would be possible in an electrically-insulating fluid. This is the basic reason that rapidly rotating stars and planets with convecting cores exhibit magnetic fields. A demonstration of this effect is seen in figure 10 where by chance the convection driven dynamo was just marginal such that it could not recover after a downward fluctuation of the magnetic field. Hence the relaxation oscillations took over from the dynamo state with their much reduced average heat flux.

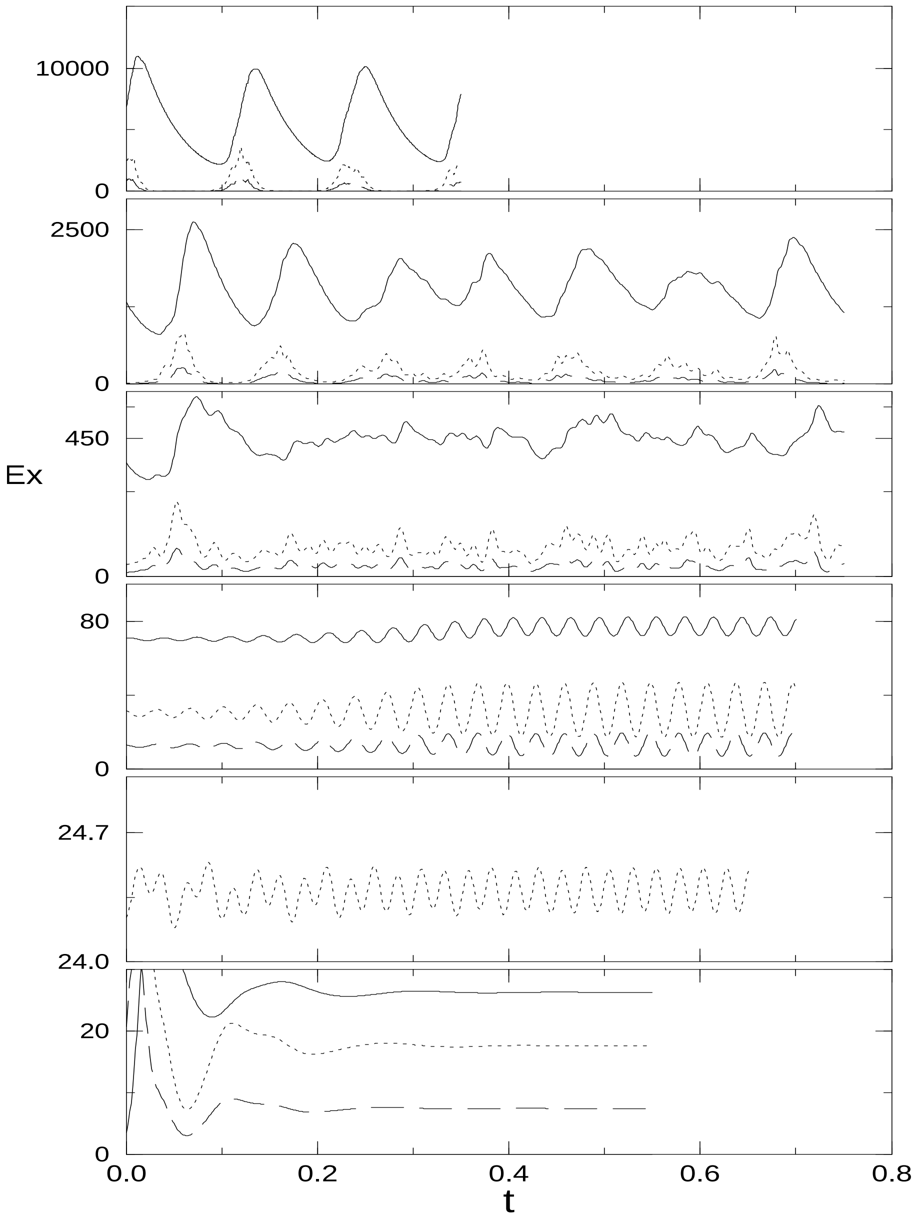

FIG. 6: Time series of energy densities of convection for $P = 0.5$, $\tau = 1.5 \times 10^4$ and $R = 3 \times 10^5$, 3.2×10^5, 3.45×10^5, 5×10^5, 7×10^5 , 10^6 , (from bottom to top). Solid, dotted and dashed lines indicate $\overline{E}_t$, $\check{E}_t$, and $\check{E}_p$, respectively. The critical Rayleigh number for onset $R_c = 215142$.

IV. TWO DISTINCT TURBULENT DYNAMOS AT IDENTICAL PARAMETER VALUES

Convection driven dynamos in rotating spherical fluid shells are often subcritical as is already indicated in figure 10 where at slightly higher Rayleigh number convection with a strong magnetic field persists, while the dynamo will decay when the magnetic field is artificially reduced to, say, a quarter of its averaged energy. There thus exists the possibility of the existence of a convection driven dynamo state and of a non-magnetic convection state at identical values of the external parameters R, τ, P, Pm where the latter parameter denotes the ratio between kinematic viscosity and magnetic diffusivity, $Pm = \nu/\lambda$. The magnetic diffusivity itself is defined as the inverse of the electrical conductivity times the magnetic permeability, $\lambda = \sigma^{-1}\mu^{-1}$.

More surprising is the fact that two different turbulent dynamo states can exist at identical values of the external parameters as has been shown in [6] and is demonstrated by the two examples shown in figure 11. Here the

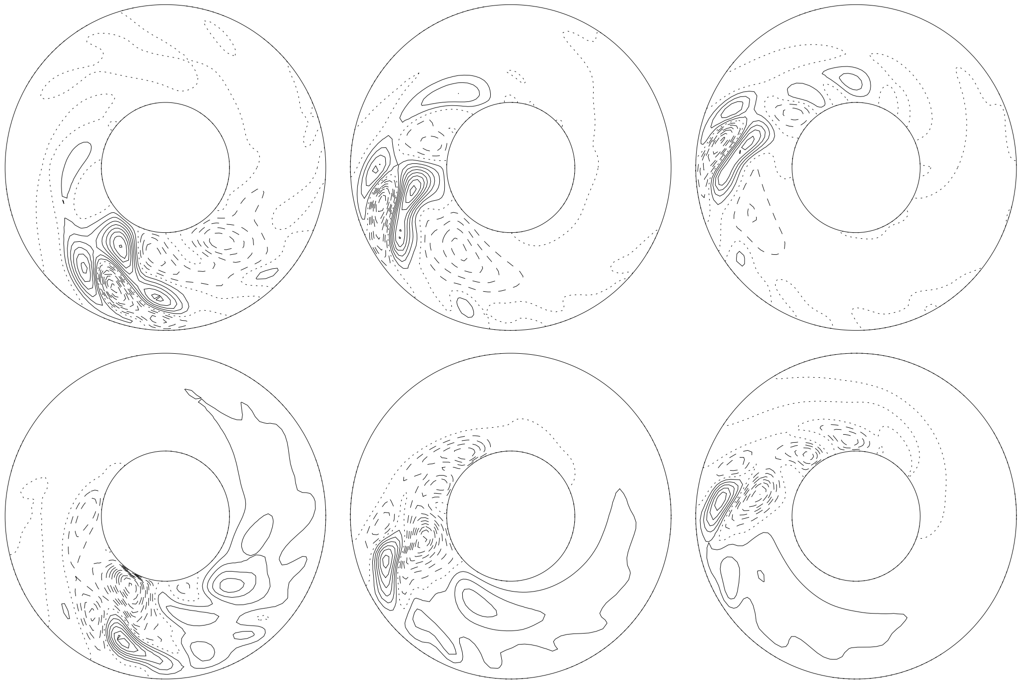

FIG. 7: Localized convection for $Ra = 7 \times 10^5, \tau = 1.5 \times 10^4, Pr = 0.5$ The streamlines, $r\partial u_p/\partial\varphi =$ const. (first row) and the isotherms, $\Theta =$ const. (second row), are shown in the equatorial plane for equidistant times (from left to right) with $\Delta t = 0.03$.

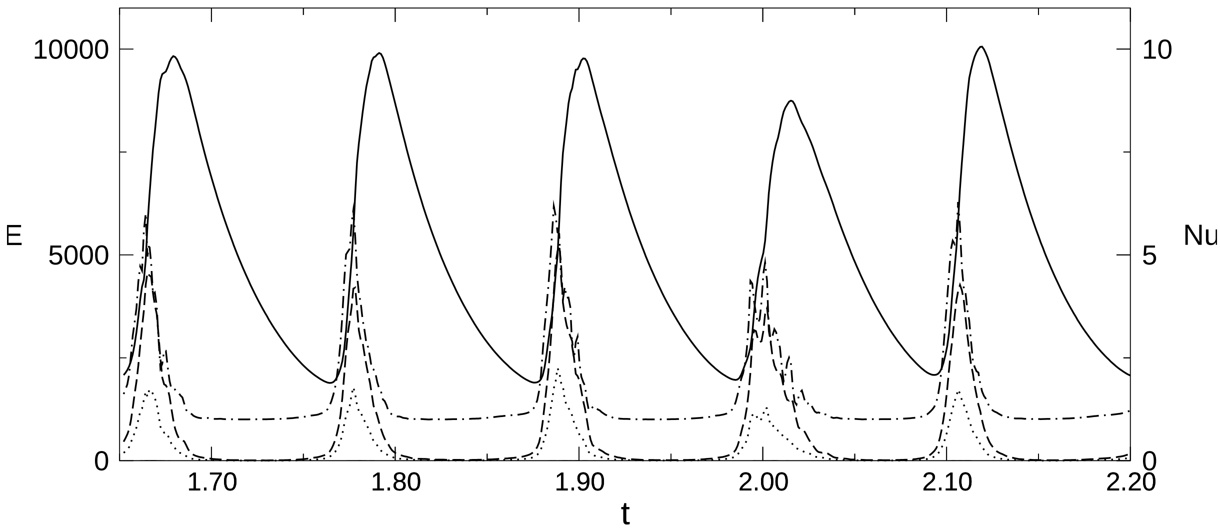

FIG. 8: Relaxation oscillations of chaotic convection in the case $\tau = 10^4, R = 6.5 \cdot 10^5, P = 0.5$. The energy densities E_t^m (solid line), E_t^f (dotted line), E_p^f (dashed line) and the Nusselt number (dot-dashed, right ordinate) are shown as function of time.

representation of the magnetic flux density $\vec{B}$ in terms of poloidal and toroidal components,

$$\vec{B} = \nabla \times (\nabla h \times \vec{r}) + \nabla g \times \vec{r} \ , \tag{4}$$

has been used and the magnetic energy densities have been defined in analogy to expressions (3),

$$M_p^m = \frac{1}{2}\langle | \nabla \times (\nabla \bar{h} \times \vec{r}) |^2 \rangle, \quad M_t^m = \frac{1}{2}\langle | \nabla \bar{g}_t \times \vec{r} |^2 \rangle \tag{5a}$$

$$M_p^f = \frac{1}{2}\langle | \nabla \times (\nabla \check{h}_p \times \vec{r}) |^2 \rangle, \quad M_t^f = \frac{1}{2}\langle | \nabla \check{g}_t \times \vec{r} |^2 \rangle. \tag{5b}$$

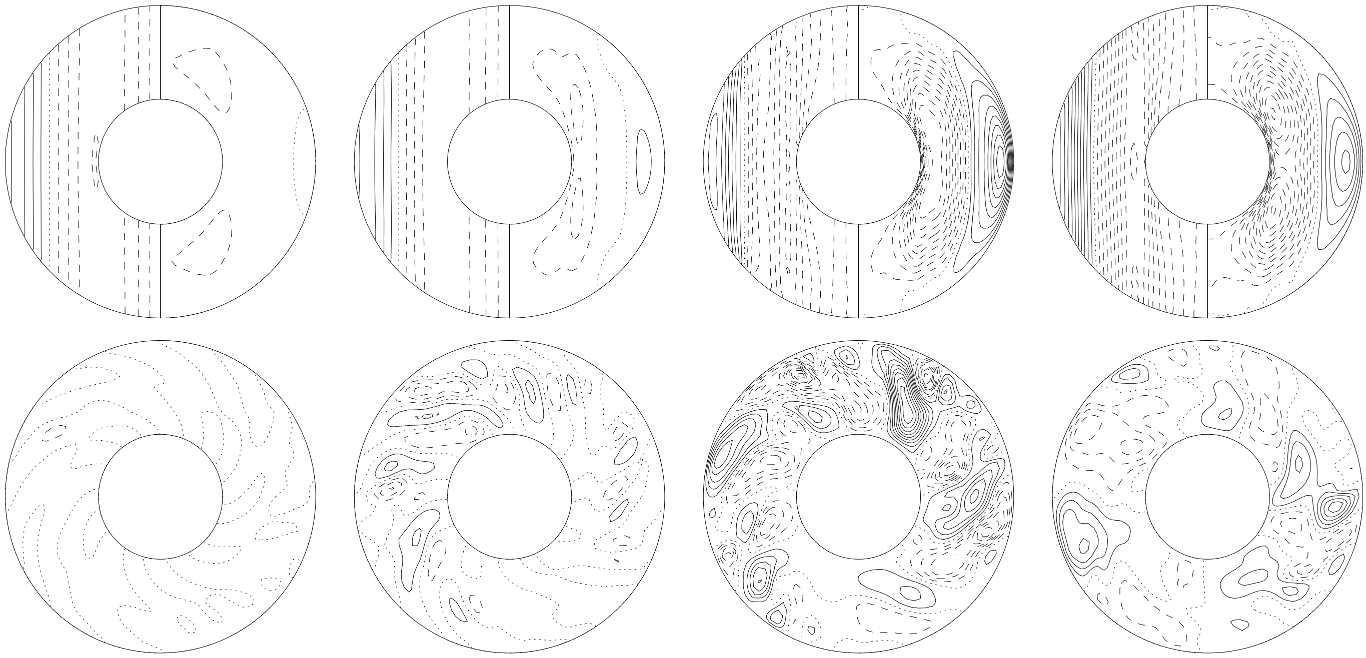

FIG. 9: Sequence of plots starting at $t = 2.31143$ and equidistant in time ($\Delta t = 0.01$) for the same case as in Fig. **??**. Lines of constant $\bar{u_\varphi}$ and mean temperature perturbation, $\bar{\Theta} =$ const. in the meridional plane, are shown in the left and right halves, respectively, of the first row. The second row shows streamlines, $r\partial u_p/\partial\varphi =$ const., in the equatorial plane.

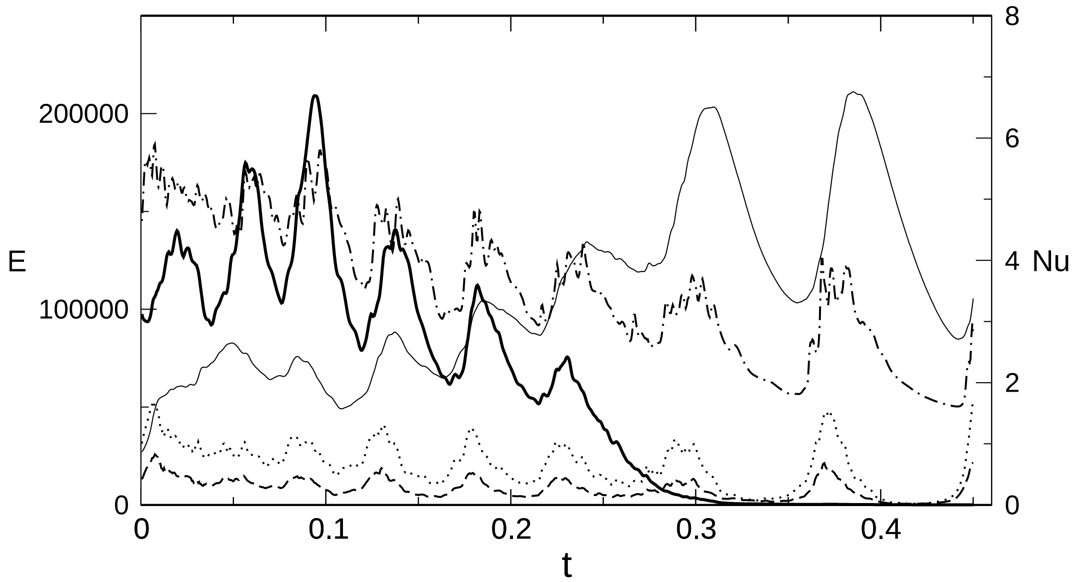

FIG. 10: Transition from a dynamo state to a state of chaotic relaxation oscillations for $\tau = 3 \cdot 10^4, R = 29 \cdot 10^5, Pm = 0.4$. The energy densities $\overline{E}_t$ (thin solid line), $\check{E}_t$ (dotted line), $\check{E}_p$ (dashed line), the total magnetic energy density multiplied by a factor 8 (thick solid line) and the Nusselt number Nu (dash-dotted line) are shown as function of time.

The two turbulent dynamo states differ strongly in their magnetic energies and their kinetic energies as is apparent from figure 11. While a strong mean poloidal magnetic field acts as an efficient brake on the differential rotation measured by E_t^m, it also inhibits convection. The alternative dynamo is characterized by a relatively weak mean magnetic field and dominant fluctuating components. Here the kinetic energy densities of convection are larger, but the differential rotation is still much weaker than in the non-magnetic case. As a result both types of dynamos provide nearly the same convective heat transport as measured by the Nusselt number Nu. This evident from figure 12 where

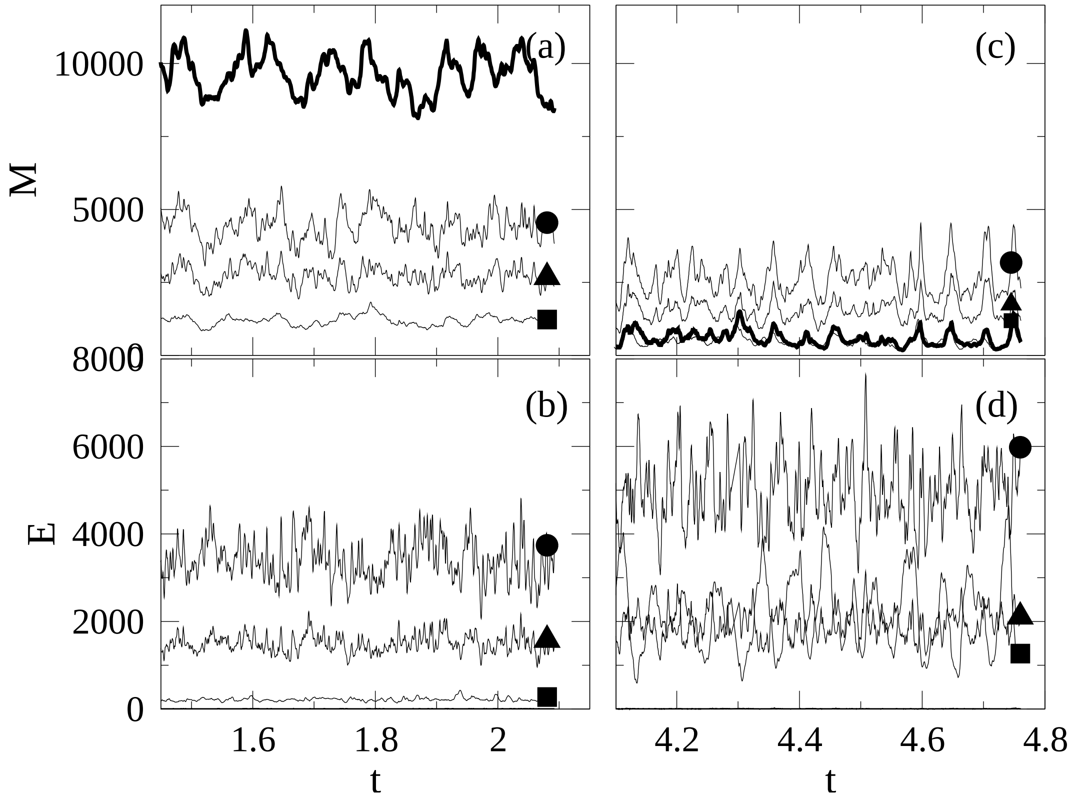

FIG. 11: Time series of two different chaotic attractors are shown - a MD (left column (a,b)) and a FD dynamo (right column (c,d)) both in the case $R = 3.5 \times 10^6$, $\tau = 3 \times 10^4$, $P = 0.75$ and $P_m = 0.75$. The top two panels (a,c) show magnetic energy densities. and the bottom two panels (b,d) show kinetic energy densities in the presence The component $\overline{X}_p$ is shown by thick solid black line, while $\overline{X}_t$, $\widetilde{X}_p$, and $\widetilde{X}_t$ are indicated by squares, triangles and circles respectively, and X stands for either M or E.

it is demonstrated that the two separate types of dynamos exist over an extended region of the parameter space.

V. CONCLUDING REMARKS

The existence of two distinct turbulent states is a rare phenomenon, although examples exist in hydrodynamics, see, for instance, [7] [8] . In magnetohydrodynamics the magnetic field offers new degrees of freedom which allow the co-existence of more than a single turbulent state. Initial conditions determine which of the competing states is actually realized.

The possibility of bistability could be of interest for the interpretation of planetary and stellar magnetism. At least this possibility should remind colleagues involved in numerical simulations of convection driven dynamos that solutions quite different from those they have obtained may exist for the same set of parameters.

Acknowledgments

The help of Dr. R. Simitev in creating the figures is gratefully acknowledged.

---

[1] E. Dormy, A.M. Soward, eds., Mathematical Aspects of Natural Dynamos, CRC Press, Taylor & Francis Group, 2007
[2] F. H. Busse, C. R. Carrigan, Laboratory simulation of thermal convection in rotating planets and stars, *SCIENCE*, **191**, 81-83 (1976)
[3] F. H. Busse, Thermal instabilities in rapidly rotating systems *J. Fluid Mech.*, **44**, 441-460 (1970)

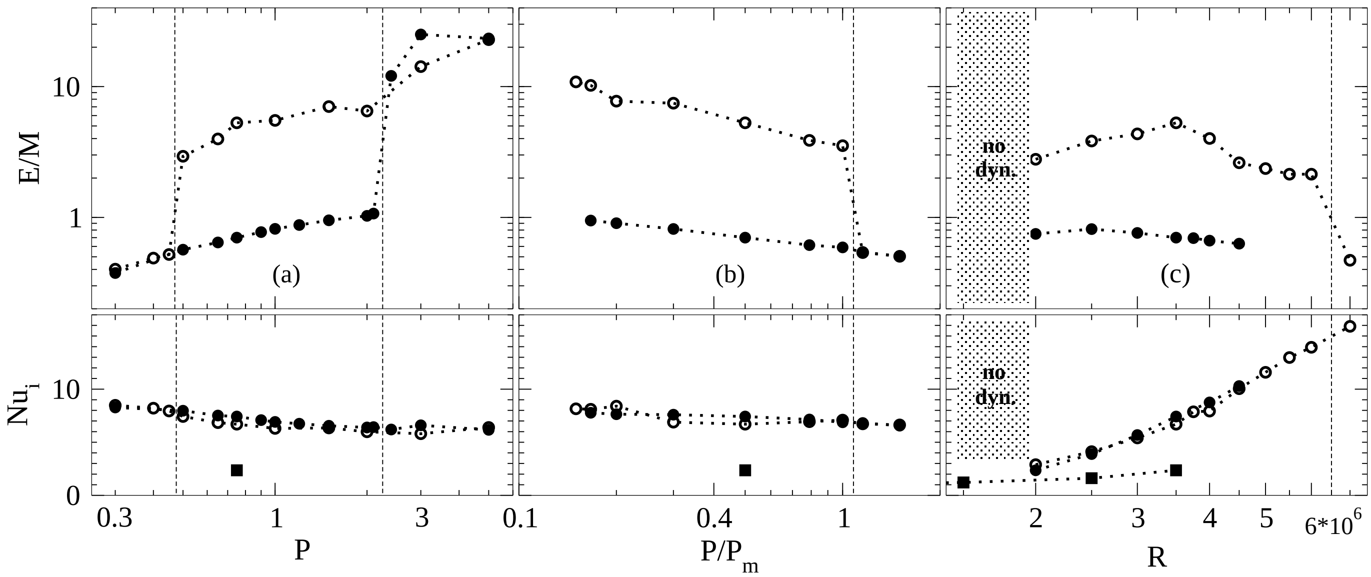

FIG. 12: The upper row shows the hysteresis effect in the ratio E/M at $\tau = 3 \times 10^4$ (a) as a function of the Prandtl number in the case of $R = 3.5 \times 10^6$, $P/P_m = 0.5$; (b) as a function of the ratio P/P_m in the case of $R = 3.5 \times 10^6$, $P = 0.75$ and (c) as a function of the Rayleigh number in the case $P = 0.75$, $P_m = 1.5$. Full full and empty circles indicate FD and MD dynamos, respectively. The critical value of R for the onset of thermal convection for the cases shown in (c) is $R_c = 659145$. A transition from FD to MD dynamos as P/P_m is decreased in (b) is expected, but is not indicated owing to lack of data. The lower row shows the value of the Nusselt number at $r = r_i$ for the same dynamo cases. Values for non-magnetic convection are indicated by squares for comparison.

[4] F. H. Busse, Asymptotic theory of convection in a rotating, cylindrical annulus. *J. Fluid Mech.*, **173**, 545-556 (1986)

[5] F. H. Busse, Convective flows in rapidly rotating spheres and their dynamo action, *Phys. Fluids*, **14**, 1301-1314 (2002)

[6] R. D. Simitev and F. H. Busse, Bistability and hysteresis of dipolar dynamos generated by turbulent convection in rotating spherical shells, *Euro Phys. Lett.*, in press **14**, 1301-1314 (2002)

[7] F. Ravelet, L. Marié, A. Chiffaudel and F. Daviaud, Multistability and Memory Effect in a Highly Turbulent Flow: Experimental Evidence for a Global bifurcation, *Phys. Rev. Lett.* **93**, 164501 (2004).

[8] N. Mujica and D. P. Lathrop, Bistability and hystreresis in a highly turbulent swirling flow, *Physica A***49**, 162-166 (2005)